SDC-92-225

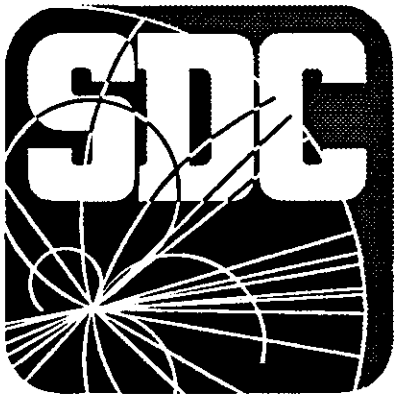

SDC
SOLENOIDAL DETECTOR NOTES

THE DESIGN OF THE CERENKOV COUNTER FOR THE SDC DETECTOR

Matt Albee, Gregory Baranko, Bruce Broomer, Mark Christoph, Mourad Daoudi, Eric Erdos, Uriel Nauenberg, Gerhard Schultz, John Smathers, Clara Wente
University of Colorado

John Belz, Gregoire Daniel, Cedric Guss, Steve Kettel, Ken McFarlane
Temple University

Ken Johns
University of Arizona

SDC-92-225

The Design of the Čerenkov Counter for the SDC Detector *

Matt Albee, Gregory Baranko, Bruce Broomer, Mark Christoph, Mourad Daoudi, Eric Erdos, Uriel Nauenberg, Gerhard Schultz, John Smathers, Clara Wente

University of Colorado, Boulder

John Belz, Gregoire Daniel, Cedric Guss, Steve Kettel, Ken McFarlane

Temple University

Ken Johns

U. of Arizona

* Research Supported by the Dept. of Energy Contract DE-AC02-86ER40253 and the Texas National Research Laboratory Commission Grant RFY9102.

Introduction. One of the characteristics of hadron colliders is the large collision rates and the associated large flux of particles at small angles relative to the beam direction ($\theta < 25°$). In the case of the SSC, preliminary conservative calculations indicate that this flux of particles can be expected to be upwards of 10^7 per sec at a luminosity of 10^{33} cm^{-2} sec^{-1} [1]. These rates will be discussed further below. These calculations do not include the effect due to the background associated with the large particle fluxes being produced inside the beam pipe and near the low radius cells of the Čerenkov counter nor the background expected from the low energy neutrons behind the calorimeter in the present detector design. This last effect is poorly known and is being measured[2]. This problem makes it difficult to design an efficient trigger system for high energy muons with the use of standard scintillator counters. In addition, these calculations show that most of this background comes from muons resulting from decays of particles produced in the jets and, as a result, their momenta in the muon detector locations are, on the average, very low (P < 10 GeV/c). As a result of these observations we propose to use a gas Čerenkov counter[3]which is very efficient in the detection of high momentum muons (P > 20 GeV/c) and completely insensitive to low momentum particles. In the SDC design we propose to use a multi-cell nitrogen gas Čerenkov counter. We now proceed to describe this element of the SDC detector.

Parameters of the SDC Čerenkov Counter. The behavior of a gas Čerenkov counter is essentially understood by the equations below which describe the angle of photon emission relative to the direction of the incident particle and the number of photoelectrons detected by a phototube on which the Čerenkov photons are incident.

$$cos(\theta_c) = \frac{1}{\beta n}$$

$$\frac{dN}{dl} = 2\pi\alpha sin^2(\theta_c) \int_{\lambda_1}^{\lambda_2} \epsilon(\lambda) \frac{d\lambda}{\lambda^2}$$

where,

β=velocity of the particle in units of the velocity of light

n=index of refraction of the Čerenkov medium = 1.000309 for N_2 gas

λ= Čerenkov photon wavelength

$\epsilon(\lambda)$ = detection efficiency of the phototube

In Fig. 1 we present the dependence of the Čerenkov angle on the particle's momentum. This angle has effectively a constant value of 24.8 mrad. In Fig. 2 we show the number of photoelectrons we expect to observe using a 5″ BURLE 8854 phototube assuming a 100 % mirror reflectivity. These results are in excellent agreement with the measured values described later on. In Table 1 we present the parameters of the design being proposed for the SDC detector.

TABLE 1
Design Parameters of the Gas Čerenkov Counter

Parameter	**Value**
Gas Medium	N_2
Gas Pressure	1 Atmosphere
Index of Refraction (λ=3500 A°)	1.000309
Width of Counter	2.00 meters
Inner Radius	2.15 meters
Outer Radius	6.55 meters
Width of Cerenkov Medium	1.85 meters
Mirror Reflectivity	85 %
Phototube	5″ BURLE 8854
Expected # of Photoelectrons	17.5
# of Cells per Counter	200
# of Mirrors per Cell	4
Size of Each Mirror	$\approx$ 40×45 cm^2
Focal Length of Each Mirror	1.40 meters
Čerenkov Light Ring Radius at Phototube	$\approx$3.73 cm
Momentum Threshold for muons	4.25 GeV/c

The operation of the counter as a trigger for high momentum muons is described in Fig. 3, where we show the alignment of a particular mirror-phototube axis relative to the beams collision point. As a muon is bent by the magnetic field in the forward toroids, the angle of incidence of the muon relative to this axis changes in proportion to the momentum. This angle would then be reflected in the number of photoelectrons produced in the phototube since the Čerenkov light ring would also move off the phototube face as indicated in Fig. 3.

Test Beam Results. In order to confirm the concepts presented here, we constructed a Čerenkov cell unit reflecting the design. This unit was then installed in Fermilab's high energy muon beam laboratory behind E-665. We carried out a series of measurements to determine the number of Čerenkov photon-electrons observed for various angles of incidence of the muons relative to the mirror-phototube optic axis. This change in angle was accomplished by placing the Čerenkov unit cell on a rotating platform. The rotation of this platform was measured to better than 0.1° by means of a sprocketed wheel attached to the rotating lead screw. A counter would detect the number of times the sprockets would pass by as the wheel rotated in unison with the platform attached to the lead screw. The mirror-phototube optic axis is so aligned that the nominal 0° occurs when the expected beam direction is normal to the cell and the Čerenkov ring is focused on the center of the phototube. Under these conditions the number of observed photoelectrons is a maximum.

In Fig. 4 we show our measurement of the linearity of the ADC relating the charge associated with the pulse and the ADC channel count. A small break in the linearity is seen at an ADC count of 50; this break is taken into account in our results stating the number of photoelectrons being detected. The performance of the Čerenkov counter was determined for two values of the Čerenkov medium length by placing a cover at a specific location inside box. This was done to check for consistency in the observed number of photoelectrons. The two lengths were 148 cm and 215 cm. In Fig. 5a we show, for a Čerenkov length of 148 cm, the single photoelectron peak measured with the counter rotated by 3.5° and 3.75°.

This measurement gives us the value the number of ADC counts and, therefore, the charge generated by a single photoelectron peak. In Fig. 5b we present the collected charge, in terms of ADC counts, for various angle of rotations. We also state the equivalent momentum that the muons would have in the SDC design to approach the Čerenkov counter at the same angle. In Fig. 5c and Fig. 5d we show the same results when the Čerenkov length was increased to 215 cm. These results clearly show the effect of the number of photoelectrons detected decreasing with angle and essentially droping to zero for angles larger than 4°. All the results presented are for clockwise rotations. We carried out a complementary series of measurements for counterclockwise rotations and obtained the same results. This reflects the similarity of the performance of the system on particles of opposite charge. These measurements lead us to the conclusion that we produce 10.2 ± 1.0 photoelectrons per meter, in excellent agreement with the calculated value. The details of this determination are shown in Table 2. These results are then used in the simulation of the counter performance as the trigger signal in the SDC detector. This is discussed in the next section.

In addition, we have measured the effect of oxygen and the effect of extending the magnetic shielding from 2″ to 4″ past the face of the phototube on the number of observed photoelectrons. The results indicate that the presence of oxygen at the level of a few percent or less does not affect the number of observed photoelectrons, even though we are coating the surface of the phototube with Pt-Phenol which enhances the detection of Čerenkov photons in the far ultraviolet. On the other hand, extending the magnetic shielding 4″ past the face of the phototube does increase slightly the number of observed photons. Hence this arrangement is incorporated in our design.

TABLE 2

Determination of Number of Observed Photoelectrons

ITEM	ADC Channel	Charge (pc)	Charge/p.e.	# of p.e.
L_c=148 cm				
Pedestal (θ=3.50°)	18.5	45.58		
Pedestal (θ=3.75°)	18.6	45.73		
Pedestal (θ=4.00°)	18.6	45.73		
Single P.E.(θ=3.50°)	21.9	50.72	5.14	
Single P.E.(θ=3.75°)	22.1	51.02	5.29	
Single P.E.(θ=4.00°)	22.5	51.63	5.90	
Ave. Charge/p.e.			5.44	
# of P.E.(θ=0.0°)	70.0	122.55		14.1±1.4
L_c=215 cm				
Pedestal (θ=3.50°)	18.3	45.28		
Pedestal (θ=4.00°)	18.1	44.98		
Single P.E.(θ=3.50°)	21.6	50.27	4.99	
Single P.E.(θ=4.00°)	22.3	49.81	4.83	
Ave. Charge/p.e.			4.91	
# of P.E.(θ=0.0°)	97.5	161.10		23.6±0.9

AVERAGE # OF P.E./METER= 10.2±1.0

Detector Simulation and Trigger Efficiency. Making use of the pulse height distribution as a function of muon incident angle measured in the Fermilab test we develop the simulation of the detector performance as a trigger counter. The Čerenkov medium in the design is about 1.8 meters. We assumed that the phototube observes 15 photoelectron for the case of a very high momentum muon instead of the expected 18 in order to err on the side of conservatism. We propagate muons through the various elements of the SDC detector including multiple scattering and energy loss. The muon is bent by the forward toroids and is then propagated into the Čerenkov counter. We use the design magnetic field of 1.8 Tesla. It is then allowed to emit the Čerenkov photons such that the observed pulse height simulates the pulse height from the number of photoelectrons generated by the phototube for such an incident muon direction. In the propagation of the photons we include the effect of spherical and astigmatic aberrations produced by the rather large spherical mirrors. We then determine, how many times the phototube observes the number of photoelectrons above a specified threshold. This method then leads to our trigger efficiency as a function of muon momentum. To describe the effect of this simulation effort[4] we show in Fig. 6a the typical Čerenkov light ring on the face of the phototube for a very high momentum, P= 300 GeV/c , a 50 GeV/c, and a 20 GeV/c muon. This case is for the center mirror in the smallest radius layer (see Fig. 8) while in Fig. 6b we show the case for a corner mirror in the largest radius layer. These 2 cases cover the extreme cases of how the Čerenkov light ring appears at the phototube face. The effect of multiple scattering is minimal compared to the toroid bending power; the multiple scattering is about 1/8 of the bend angle and this ratio is independent of momentum. The multiple scattering effect is clearly seen in the increasing spread of the 50 GeV/c and 20 GeV/c light ring when compared with that of the 300 GeV/c ring. The scatter in the 300 GeV/c ring is due mainly to spherical aberrations. From these two diagrams we note that the detection efficiency versus momentum is very similar to the point that the trigger effciency versus momentum is the same for all mirrors.

In Fig. 7a we display the simulated trigger efficiency versus momentum. The

two curves are for extreme threshold requirements. This gives one a sense of the dynamic range in trigger rates available for this design. In Fig. 7b we show the same trigger efficiency versus the transverse momentum for the five radial layers of mirror cells (see Fig. 8). These results are then used to determine the trigger rate. We use the results of the work of Green and Hedin[1] which present the cross section for a muon to appear beyond a certain amount of material versus transverse momentum and versus angle. In Table 3 below we present the trigger rates expected under the present design. This design can be altered by the addition of Winston cones which allows one to reach smaller values of transverse momentum in the outer layers if one desires to have a more universal trigger efficiency versus transverse momentum than that shown in Fig. 7b. Since the outer layers have a low trigger rate this addition would not alter significantly the results presented in Table 3. Such a possibility is discussed in a latter section.

TABLE 3

Trigger Rates Summed Over Both Ends

Trigger Rate per Octant = 1/16

Luminosity = 10^{33} cm^{-2} sec^{-1}

Layer Radius (m)	θ(deg.)	η	Trigger Rate
2.64	9.4	2.50	2.3×10^{3}
3.55	12.5	2.21	1.1×10^{3}
4.46	15.6	1.99	4.1×10^{2}
5.37	18.6	1.81	1.6×10^{2}
6.28	21.5	1.66	9.2×10^{1}

These trigger rates are quite low. They are not affected by the low energy charge particle debris that is associated with the back of calorimeters or materials

that are placed in the path of charged tracks. This is because of the properties of Čerenkov counters; namely, light is only emitted by relatively high momentum tracks (P>4.3 Gev/c for muons and P> 21 MeV/c for electrons) and the light must be within a 5° cone of a direct line from the target. In addition, it is totally insensitive to a flux of low energy neutrons which might be quite intense in the forward direction.

Mechanical Structure of the Čerenkov Counters. In this section we describe the structure and dimensions of the counter. The counter in each end is divided into eight sections (octants) located radially and perpendicular to the beam line. In Fig. 8 we show a frontal schematic view of such a unit where we show the mirror structure and location of the 25 phototubes, each phototube observing four mirror cells. The location of the phototube relative to its 4-mirror cell is located so as to minimize spherical and astigmatic aberrations. The distance from the interaction point to the mirror plane is $\approx$ 16 meters. The depth of each octant is $\approx$ 2 meters and the volume is 3.9 m^3.

All eigth octants attach to a "spider", a welded structural frame made of Aluminum I-beams. This frame is shown in Fig. 9. The estimated weight of this structure is 2700 lbs. We plan to have dowells on the spider for precision mounting of the octants. These dowells will have bearings to allow for some motion of the octant for alignment purposes. This system will assure precision positioning of the octants. The spider and the octants are joined on the downstream side. The octants will have removable panels as described below. The assembly of the octant and spider will still allow for the removal of the panels in situ. The octants on the upstream side will be bracketed together to add to the rigidity of the structure. The bracketing will occur on the inner and outer radius.

The octants are constructed as a frame made of structural angle and welded panels (2 sides, top, and bottom). Both frame and panels make up the integral, rigid part of the structure. Each side has flanged opening ports. These ports are necessary to service the photomultipliers and mirrors. The panels consist of a 1″

honeycomb-aluminum sheet laminates. They are ≈ 4 m^2 and weigh 125 lbs. Each panel has a flange around its periphery which mates with the flange making up the ports. A flat rubber gasket between the panel flange and the port flange will seal the opening when the two are mated. The estimated weight of each octant , with the mirror weight included, is 4300 pounds.

The panels covering the outer element of the octants will have a gastight recessed utility trough. This trough is located in the upstream inactive region of each octant so as not to project a shadow on the mirrors and affect the Čerenkov light collection. The dimension of the trough is 300 cm. in length, 50 cm. in width, and 20 cm. deep. It will accomodate the gas supply and return connections, provide high voltage connection to the phototube and the output signal connections. In addition, it will have ample space for the location of the front end electronics. Each one of these troughs will service the 25 photomultipliers in the octant.

In the interior of each octant, parallel to the upstream and downstream sides, separated by about 190 cm., are tubular weldments. They consist of 5 horizontal and 3 vertical pipes. These are shown in Fig. 10. The horizontal pipes will hold the phototube assemblies and cables on the upstream side, and the mirror assemblies on the downstream side. The vertical pipes serve as stiffeners, specially on the downstream side, where the mirrors are located. There are 25 photomultipliers and 100 mirrors per octant as shown in Fig. 8. The diameter of the pipes are 2.0″ o.d. by 0.25″ wall, designed at present to hold only 3 mm. thick glass. The total weight of the glass is 280 lbs. In addition, the hardware to hold the mirrors in place adds about 500 lbs. If thicker glass is needed then thicker support pipes will be required on the downstream side only. The holders for the phototubes and mirrors will allow us to adjust orientations in x, y, and z and will incorporate rotational capabilities. This will permit maximal adjustment of the photomultipliers and the mirrors to obtain good focus location. The spacing between the mirror plane and the photomultiplier plane is about 140 cm. A 3-d view of the structure is shown in Fig. 11

The counter will run at atmospheric pressure. Assuming an operating pressure of $0.5''$ of water above atmospheric pressure the net average force on a side is $\approx$ 500 lbs.

Alignment We need to maintain an active alignment mechanism that will allow us to detect, for every octant, angular deviations of a fraction of a degree. Our present design is shown in Fig. 12. It consists of arrays of 4 light detecting diode cells on each outermost corner of an octant structure that observes a small light beam emitted by a light source with a focusing lens attached to elements of the beam pipe. This light-lens structure is carefully surveyed to be perpendicular to the beam line. A deviation of $0.25°$ over a distance of 4 meters leads to a light spot displacement of 1.7 cm, easily observable by the 4 diode structure. By observing the size of the pulse signal from each of the 4 diodes we can easily maintain the alignment of each octant relative to the beam line.

Possible Improvements One simple future addition to the present design is to add Winston cones to the two outermost or more layers. One such cone is shown in Fig. 13. The max. angle of incidence of the Čerenkov light on the surface of the Winston cone for the present design is $27°$ so that a $35°$ Winston cone allows for a high collection efficiency. This Winston cone increases the detection radius from 6.3 cm. to 11 cm. or less depending on the length of the cone. This allows us to reduce the threshold for the outermost layers shown in Fig. 7b from 8 GeV/c to $\approx$ 4.6 GeV/c or higher. Similarly for the next to the outermost layer, by using a slightly shorter Winston cone. Since the trigger rates are already low, adding these does not affect the basic low trigger rate behavior of the counter.

The present design trigger using the Čerenkov counter requires that each cell be placed in coincidence with a scintillator cell that corresponds in dimension to the Čerenkov cell or with the beam clock in case the scintillator cell has too much background. The singles rate of the Čerenkov phototube due to its dark current has measured to be 100 Hz. Such a rate when placed in coincidence with the beam clock leads to an accidental trigger rate of $\approx$ 100 Khz which is far higher that the

actual trigger rate due to muons as presented in Table 3. One solution we proposed is shown in Fig. 14. It consists of using 4 2″ phototubes that cover the Čerenkov light ring. The Čerenkov signal for the trigger is the coincidence between any two or more of the phototubes. This then reduces the singles rate from the Čerenkov unit to a negligible amount, $\approx 10^{-4}$ instead of 100 Hz. This reduces the trigger rate, using the beam counter as the other signal, to a negligible level. The efficiency of this trigger as a function of the muon momentum is shown in Fig. 15 and we note that we hardly loose any efficiency when compared to the trigger efficiency using 1 phototube which is shown in Fig. 7a. For completeness we also present the trigger efficiency if we demand a coincidence of three or more phototubes. It is quite clear that this phototube arrangement is effective in reducing the accidental tirgger rates while maintaining the high efficiency at moderate values of P_t.

REFERENCES

1. Muon Rates at the SSC, Dan Green, David Hedin, Nuc. Inst. and Meth. A297, (1990) 111-120. Rates for Triggers, SDC-90-00075, Dan Green.
2. Ken Johns U. of Arizona. Measurements being carried out at Fermilab.
3. We would like to thank Michael Marx for his comments to us that lead us towards the present design.
4. These rings are the overlay of many tracks that strike the reflecting mirrors so as to cover the area of the 4 associated with one cell. Hence the number of photoelectrons seen in the Figure is much larger than the nominal 17 per muon.

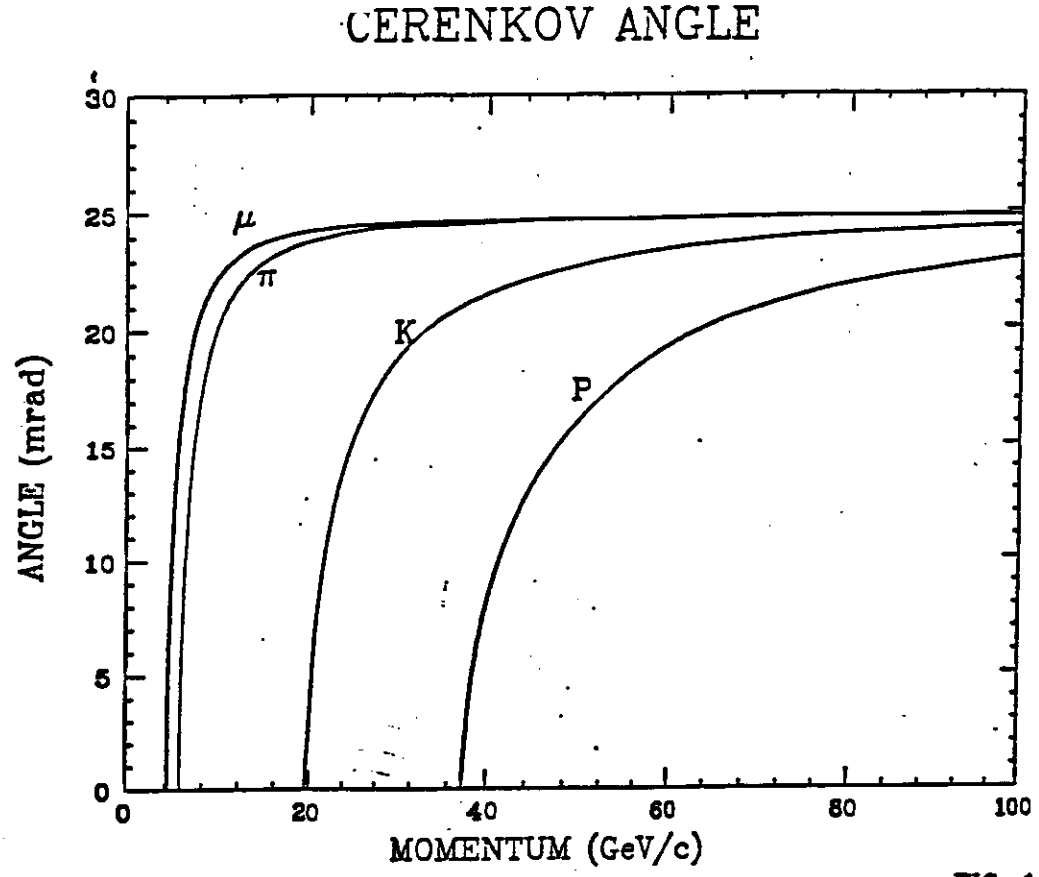
ČERENKOV ANGLE
ANGLE (mrad)
MOMENTUM (GeV/c)
μ
π
K
P
0
5
10
15
20
25
30
0
20
40
60
80
100

FIG. 1

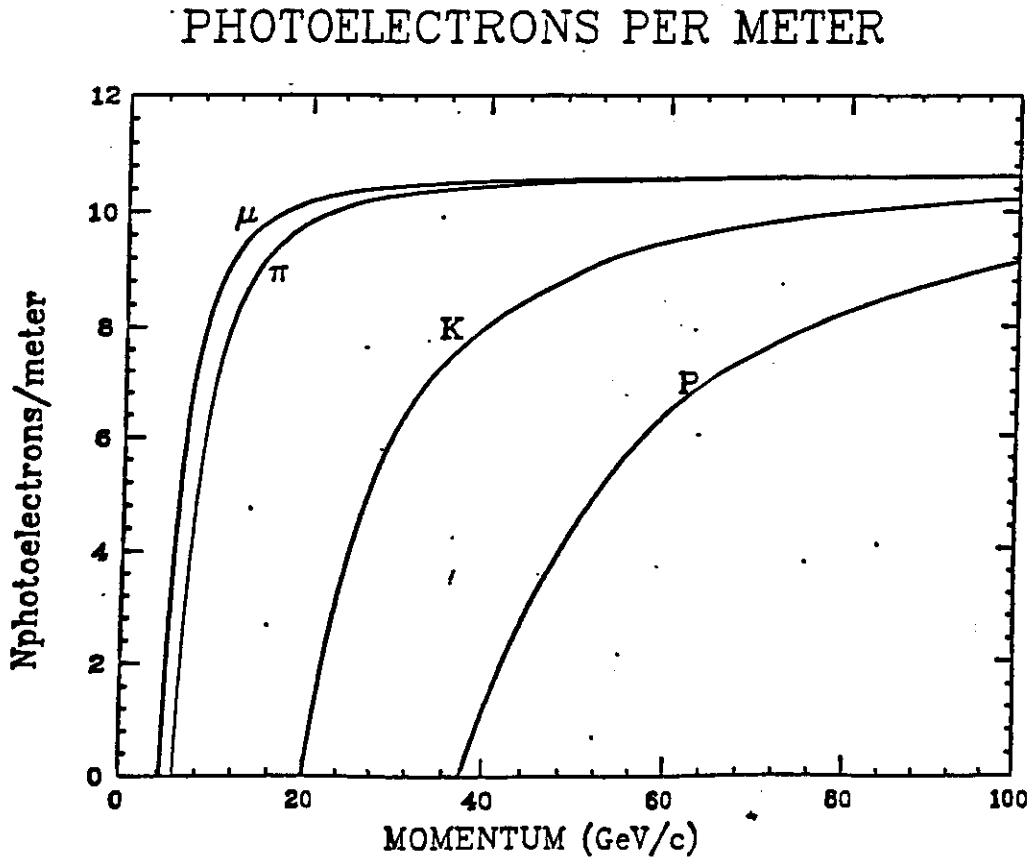
PHOTOELECTRONS PER METER
Nphotoelectrons/meter
MOMENTUM (GeV/c)
μ
π
K
P
0
2
4
6
8
10
12
0
20
40
60
80
100

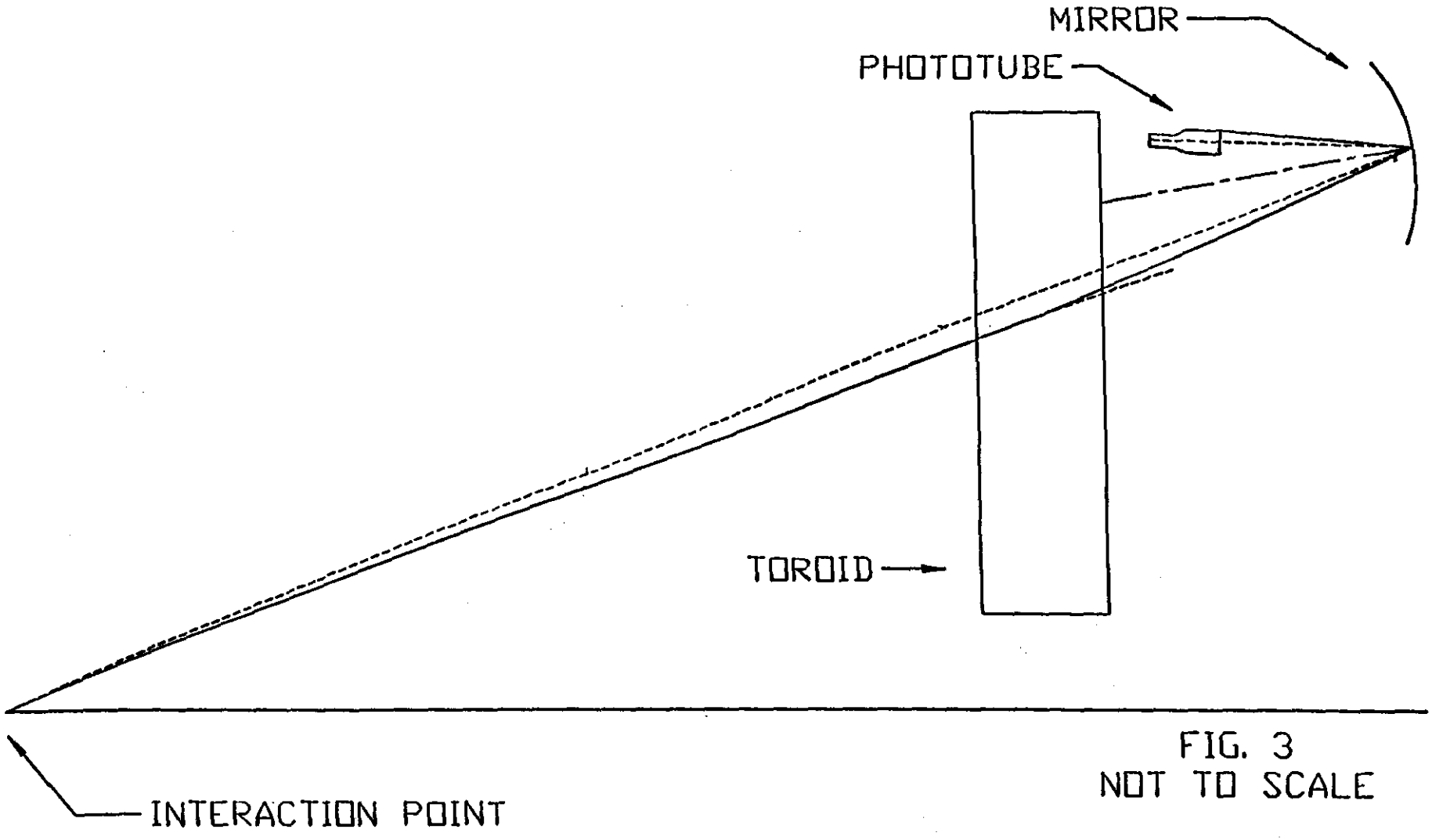

FIG. 3
NOT TO SCALE

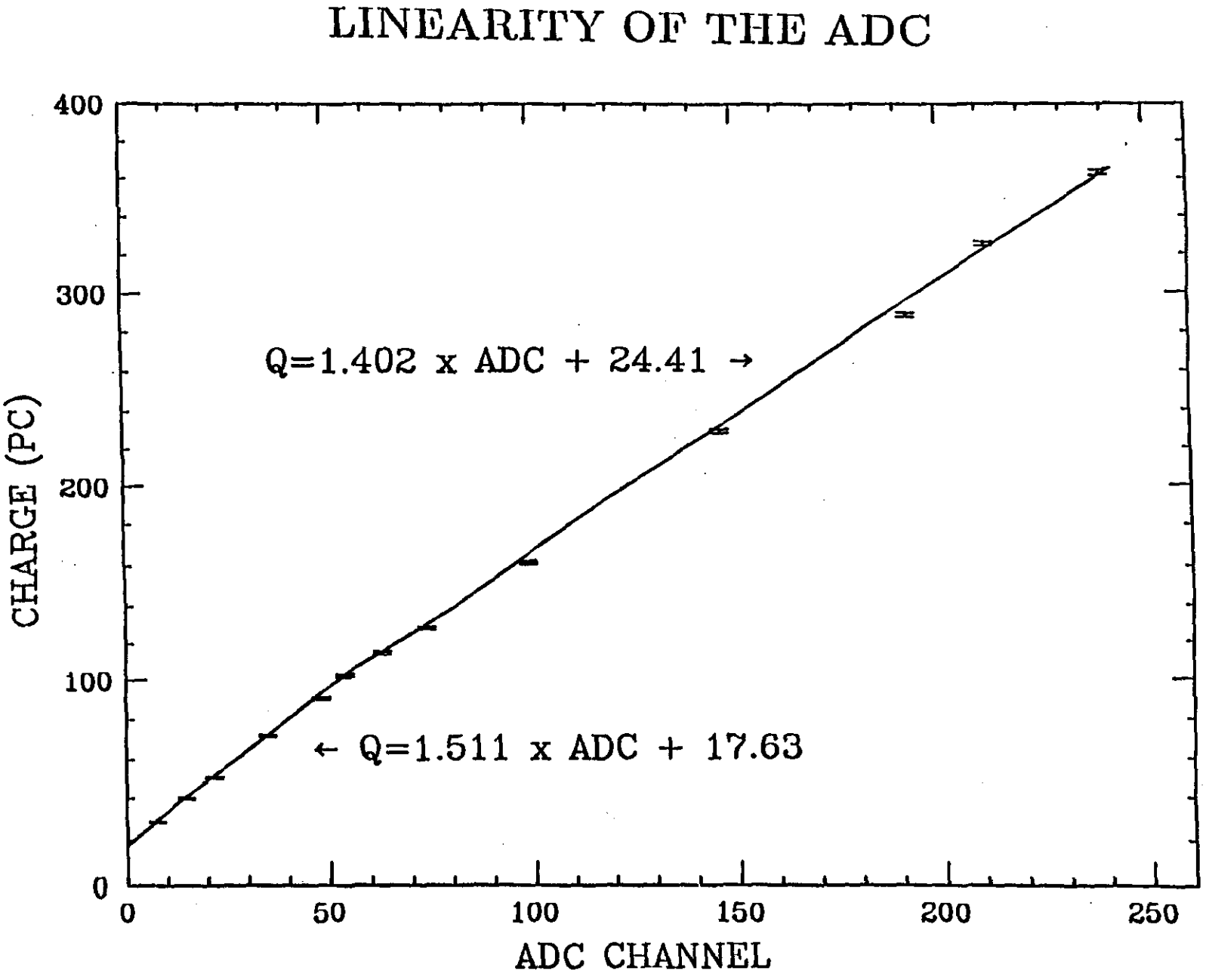
LINEARITY OF THE ADC
400
300
200
100
0
CHARGE (PC)
Q=1.402 x ADC + 24.41 →
← Q=1.511 x ADC + 17.63
0
50
100
150
200
250
ADC CHANNEL

FIG. 4

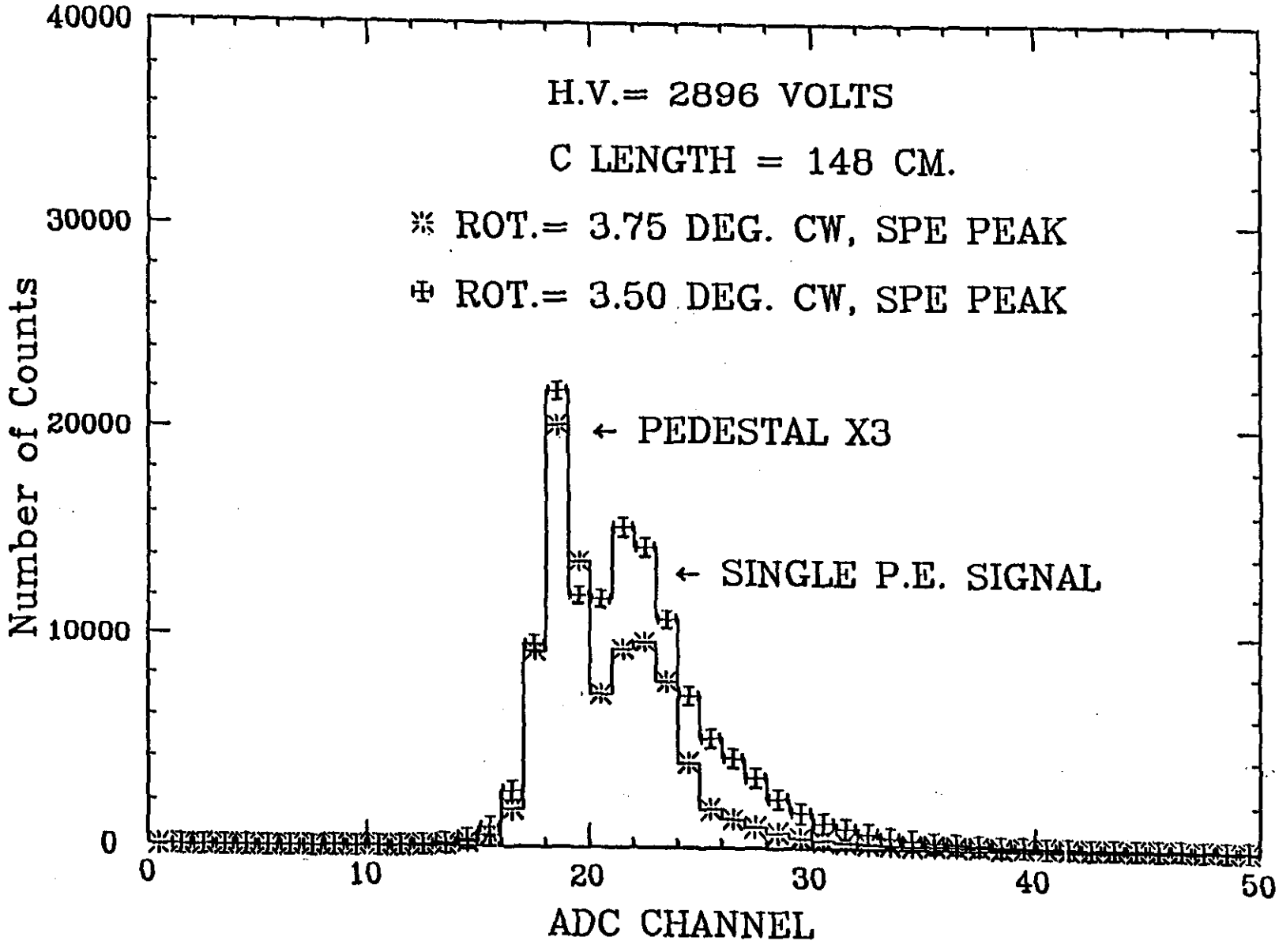
H.V.= 2896 VOLTS
C LENGTH = 148 CM.
ROT.= 3.75 DEG. CW, SPE PEAK
ROT.= 3.50 DEG. CW, SPE PEAK
← PEDESTAL X3
← SINGLE P.E. SIGNAL
Number of Counts
ADC CHANNEL
0
10000
20000
30000
40000
0
10
20
30
40
50

F 5a

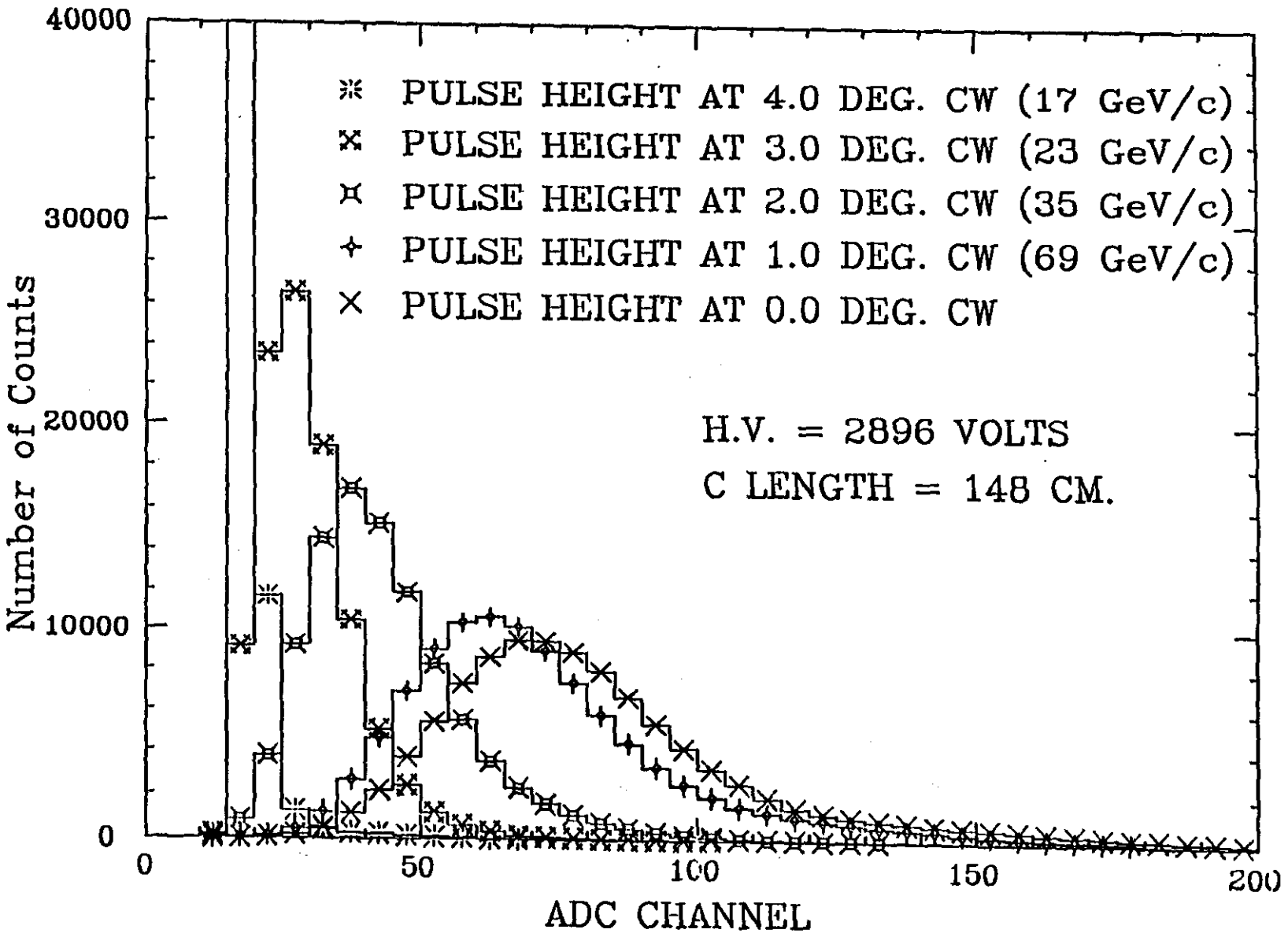
40000
30000
20000
10000
0
Number of Counts
0
50
100
150
200
ADC CHANNEL
PULSE HEIGHT AT 4.0 DEG. CW (17 GeV/c)
PULSE HEIGHT AT 3.0 DEG. CW (23 GeV/c)
PULSE HEIGHT AT 2.0 DEG. CW (35 GeV/c)
PULSE HEIGHT AT 1.0 DEG. CW (69 GeV/c)
PULSE HEIGHT AT 0.0 DEG. CW
H.V. = 2896 VOLTS
C LENGTH = 148 CM.

FIG. 5b

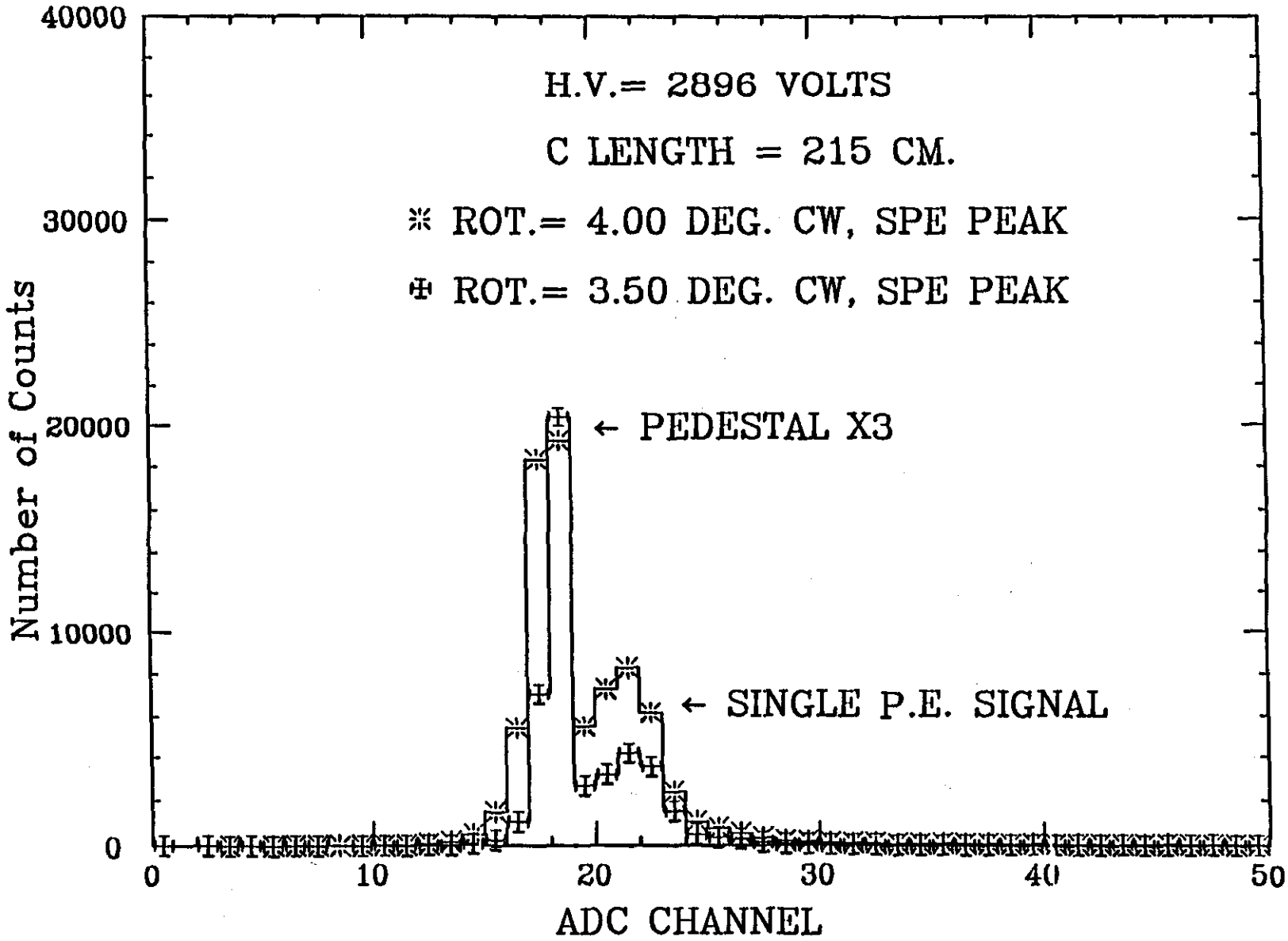
H.V.= 2896 VOLTS
C LENGTH = 215 CM.
ROT.= 4.00 DEG. CW, SPE PEAK
ROT.= 3.50 DEG. CW, SPE PEAK
← PEDESTAL X3
← SINGLE P.E. SIGNAL
Number of Counts
ADC CHANNEL
40000
30000
20000
10000
0
0
10
20
30
40
50

F 5c

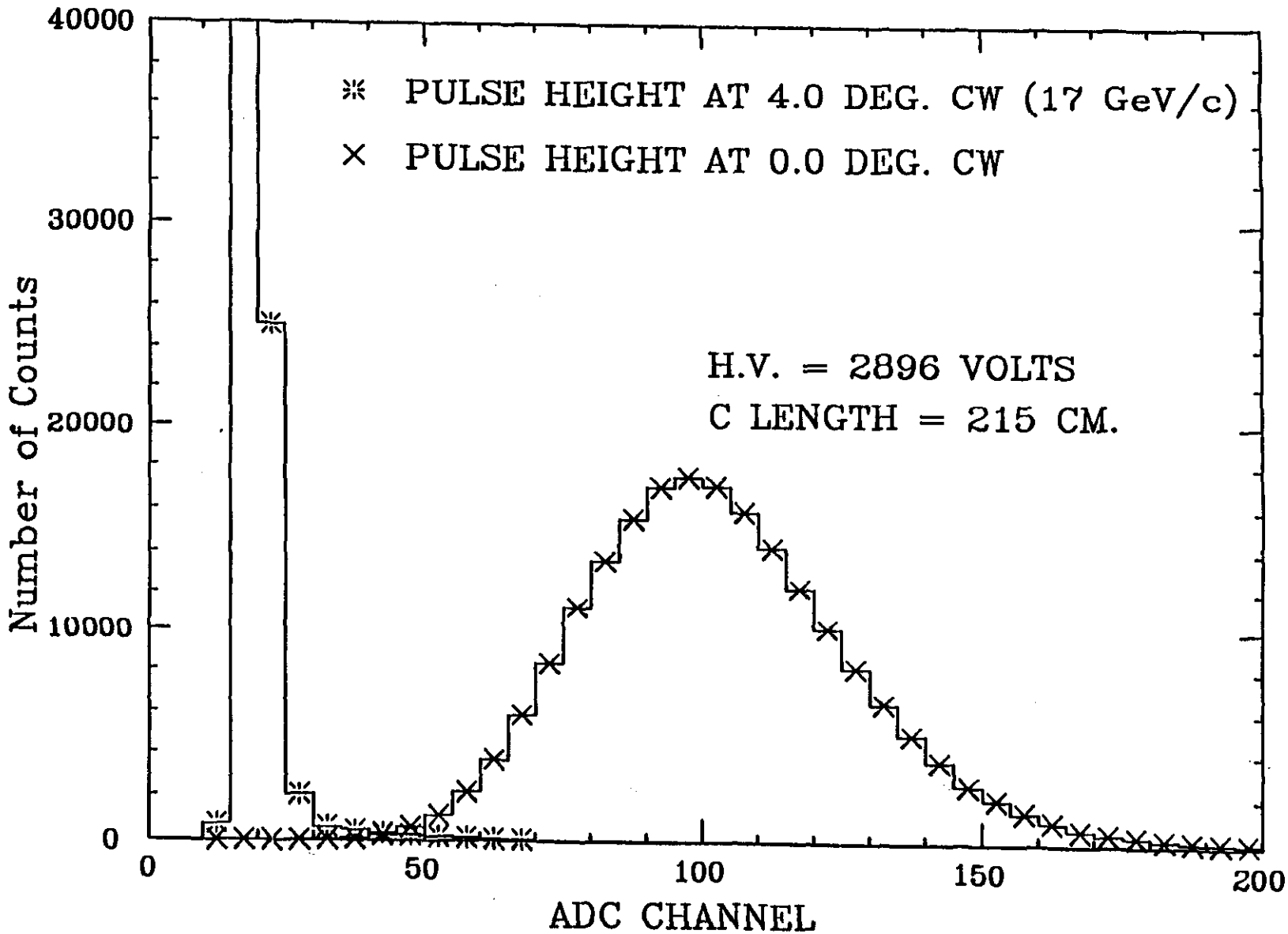
40000
30000
20000
10000
0
Number of Counts
PULSE HEIGHT AT 4.0 DEG. CW (17 GeV/c)
PULSE HEIGHT AT 0.0 DEG. CW
H.V. = 2896 VOLTS
C LENGTH = 215 CM.
0
50
100
150
200
ADC CHANNEL

FIG. 5d

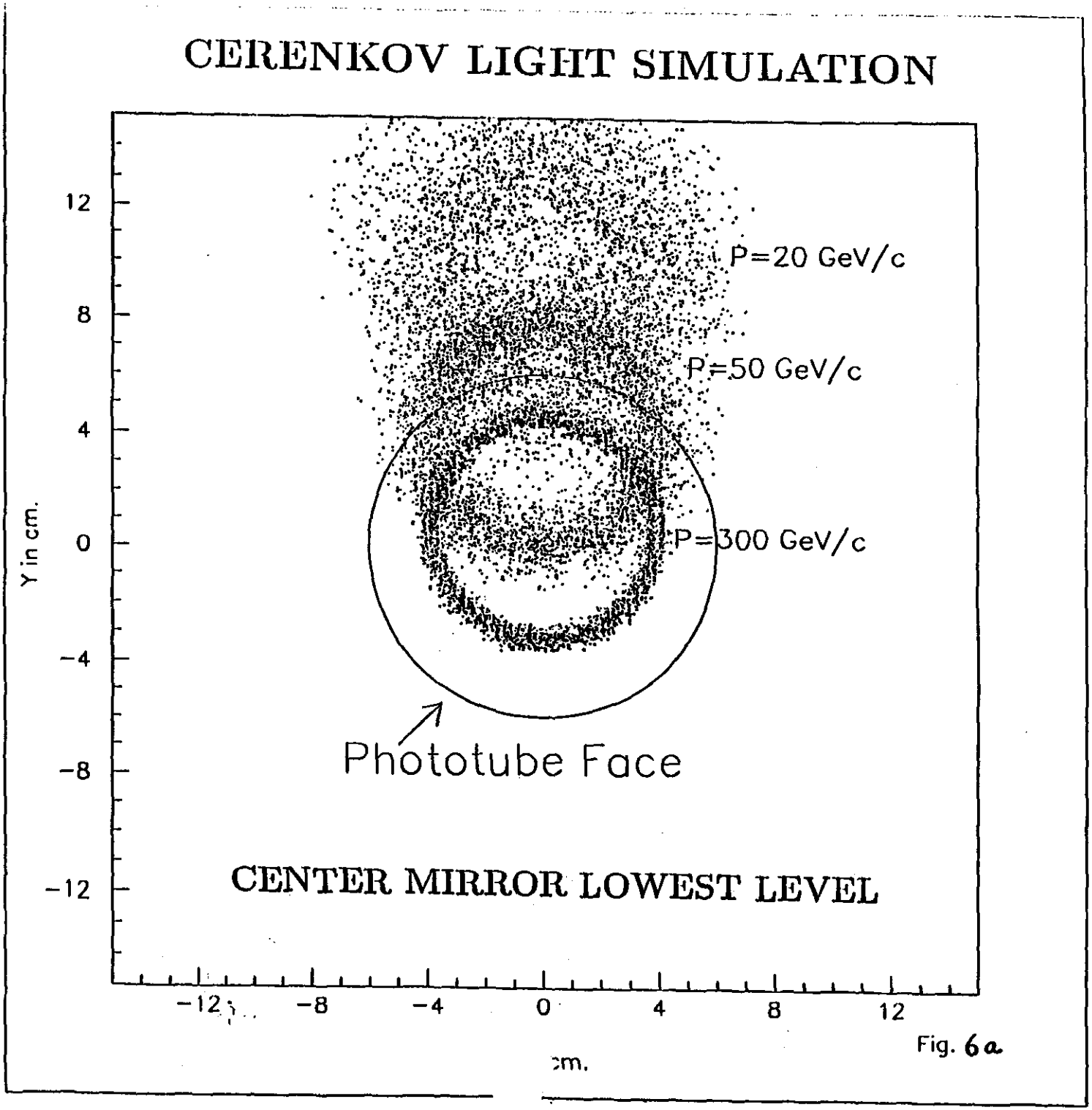
CERENKOV LIGHT SIMULATION
P=20 GeV/c
P=50 GeV/c
P=300 GeV/c
Phototube Face
CENTER MIRROR LOWEST LEVEL
Y in cm.
12
8
4
0
-4
-8
-12
-12
-8
-4
0
4
8
12
cm.

Fig. 6a

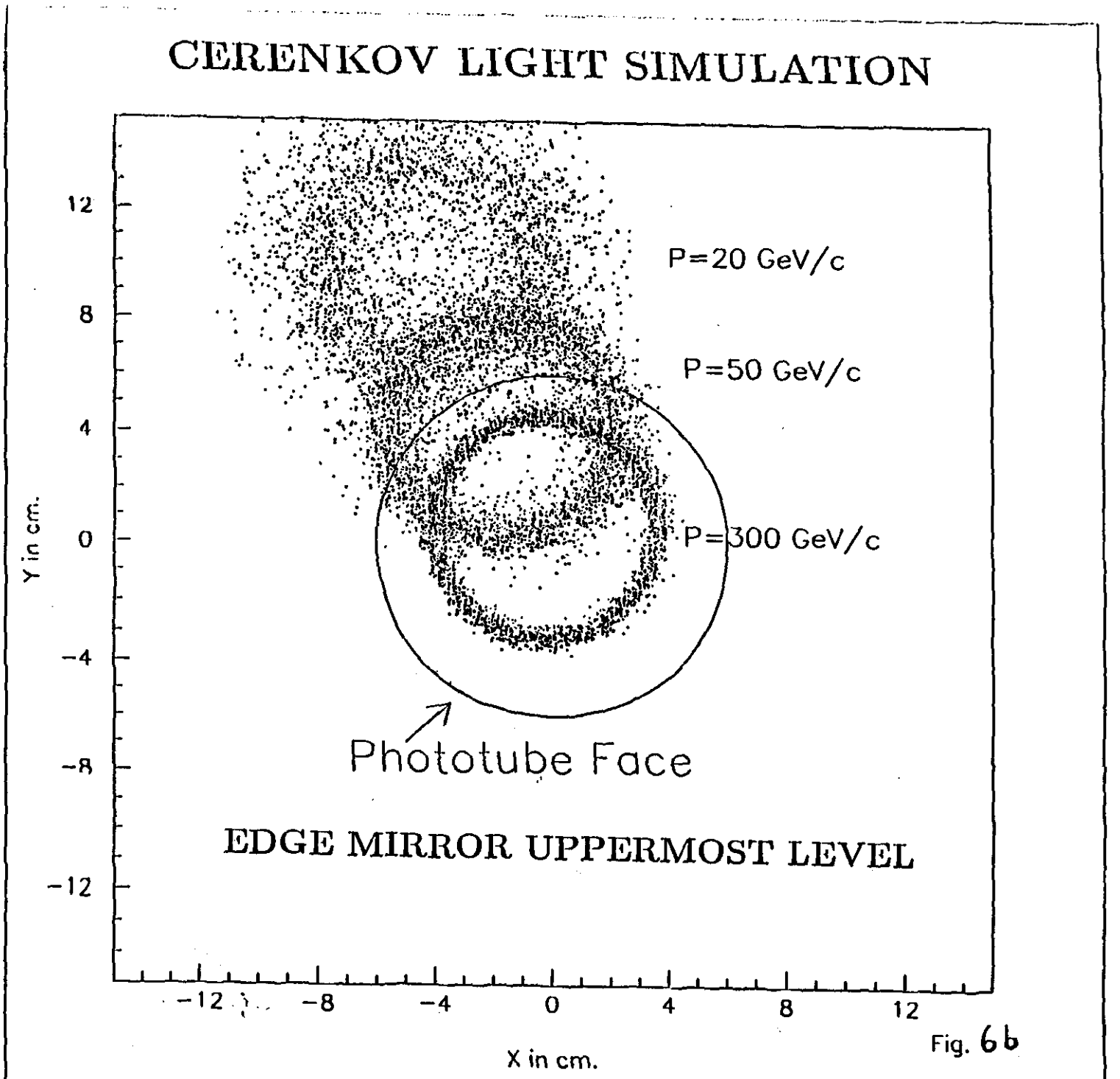
CERENKOV LIGHT SIMULATION
P=20 GeV/c
P=50 GeV/c
P=300 GeV/c
Phototube Face
EDGE MIRROR UPPERMOST LEVEL
Y in cm.
X in cm.
12
8
4
0
-4
-8
-12
-12
-8
-4
0
4
8
12

Fig. 6b

TRIGGER EFF. VERSUS MOMENTUM

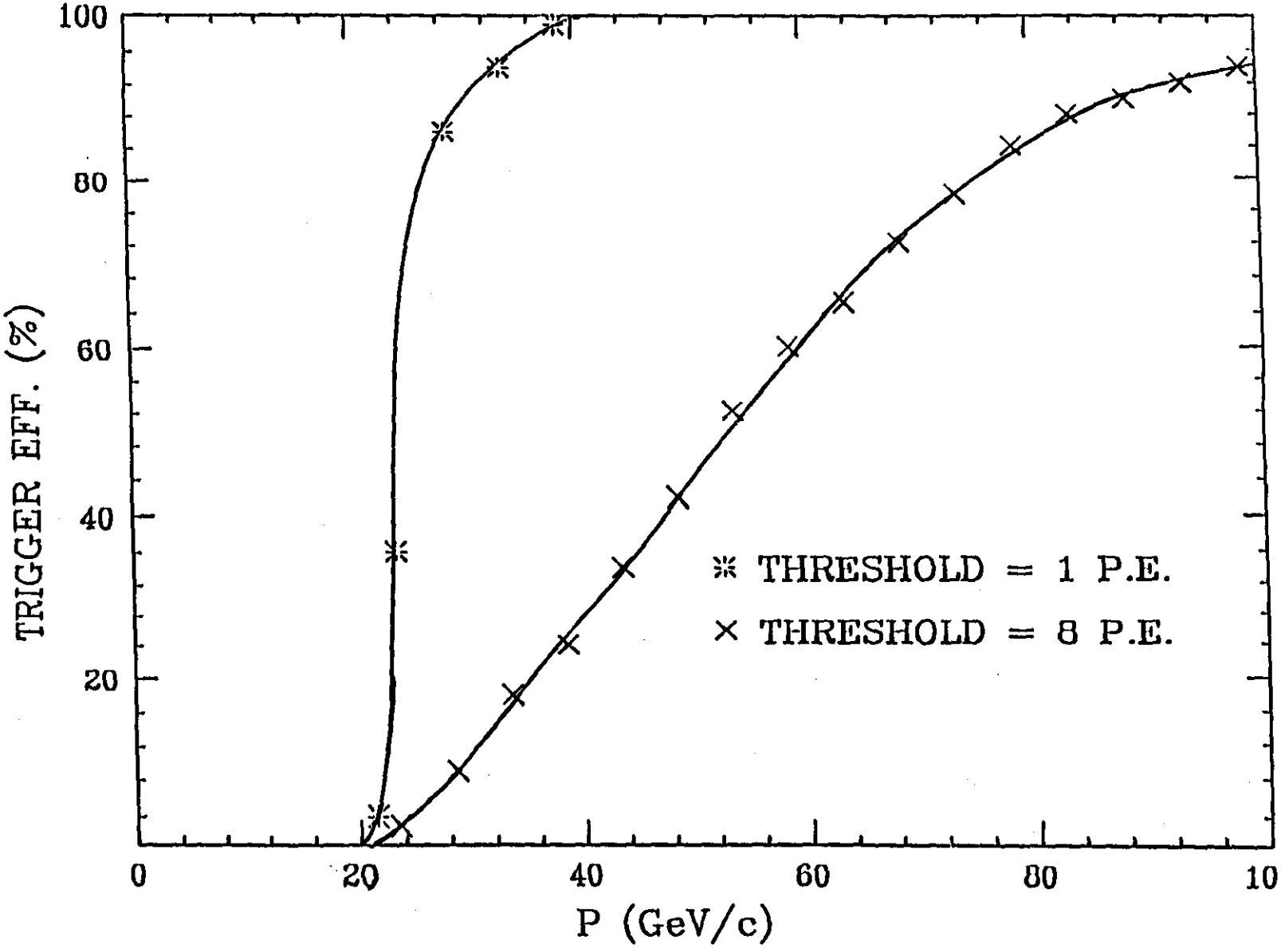

Fl 7a

TRIGGER EFF. VERSUS TRANS. MOMENTUM

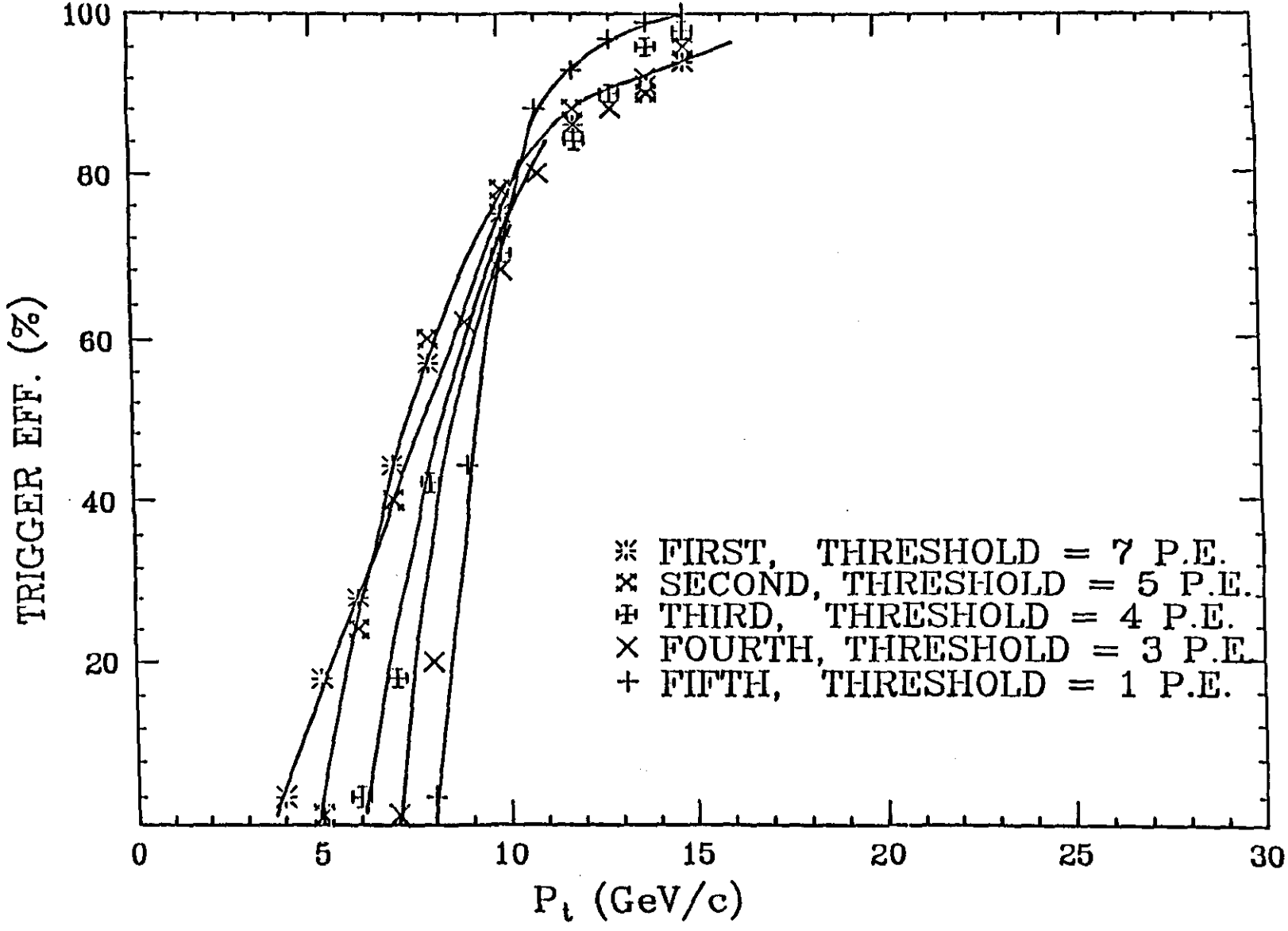

FIG. 7b

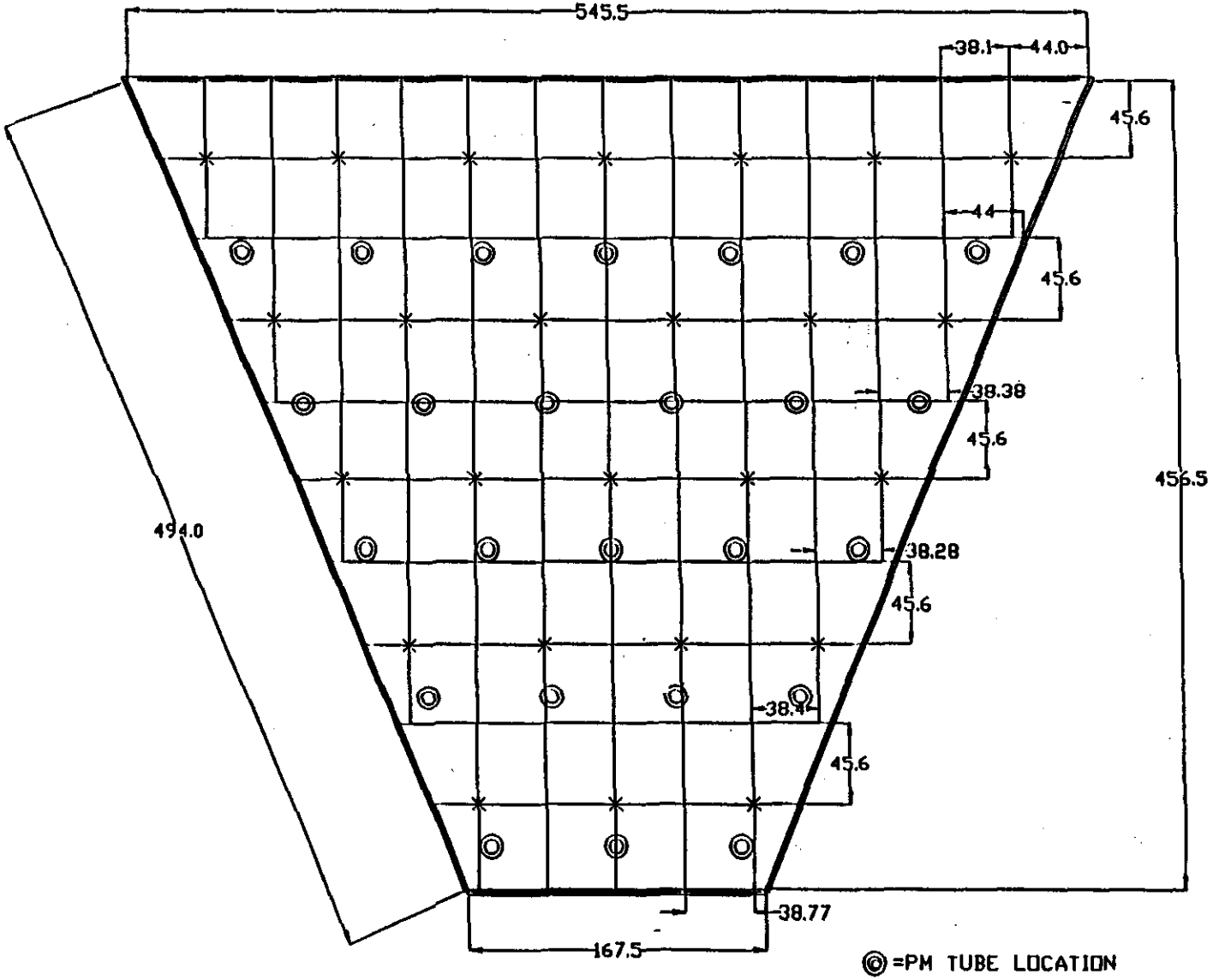
545.5
38.1
44.0
45.6
44
45.6
38.38
45.6
456.5
494.0
38.28
45.6
38.4
45.6
38.77
167.5
◎=PM TUBE LOCATION
x=4 MIRROR GEO.CENTER

FIG.8

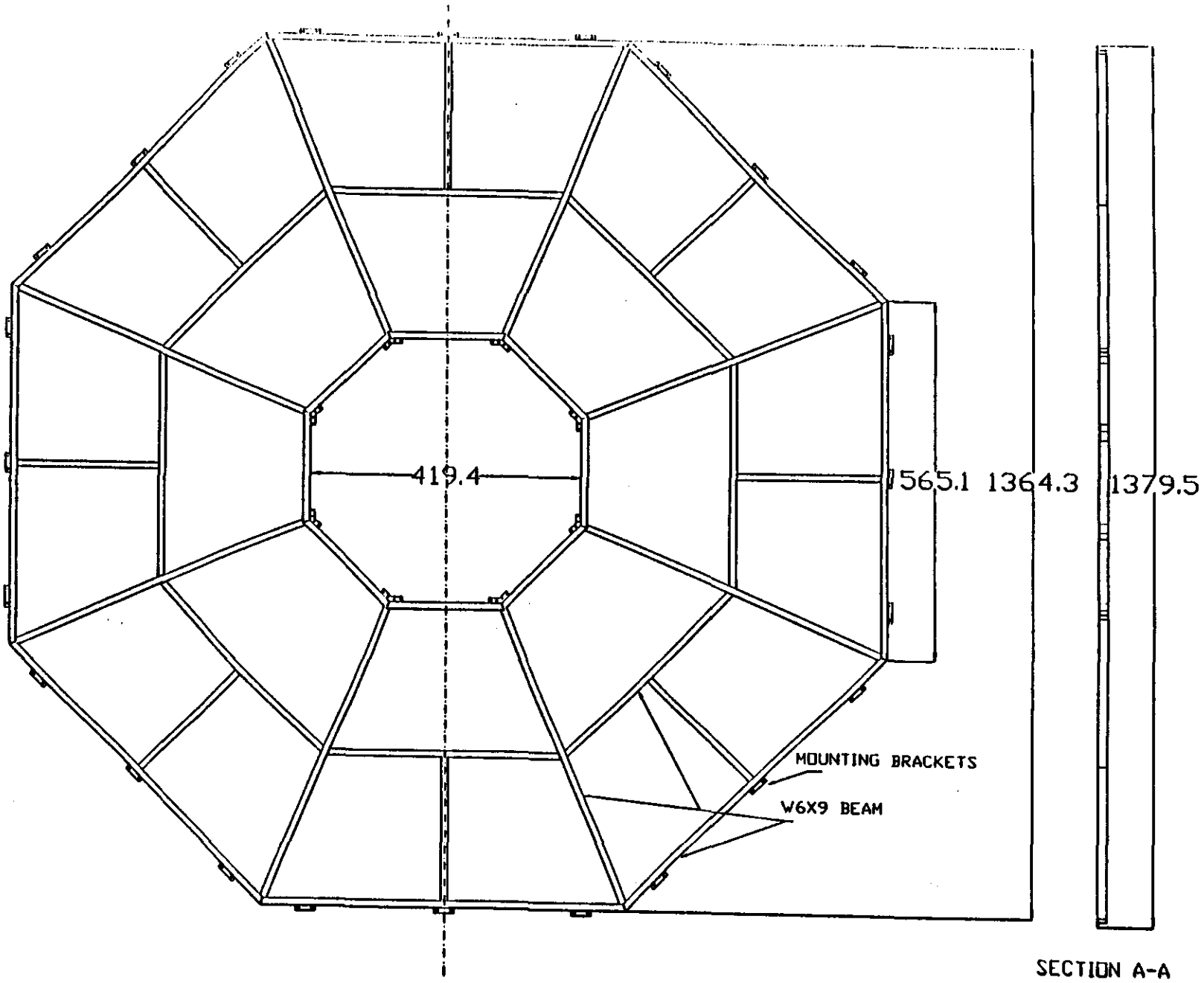

SPIDER-FRAME ASSEMBLY
U. OF COLORADO

NOT TO SCALE
DIM.IN CM

FIG.9

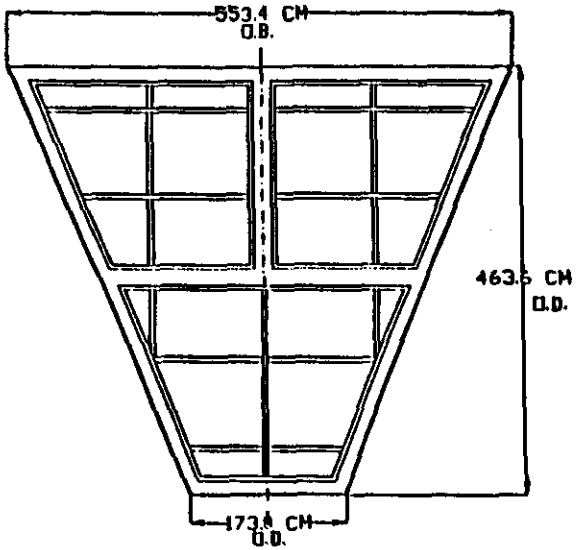

FRONT-VIEW
(COVERS REMOVED)

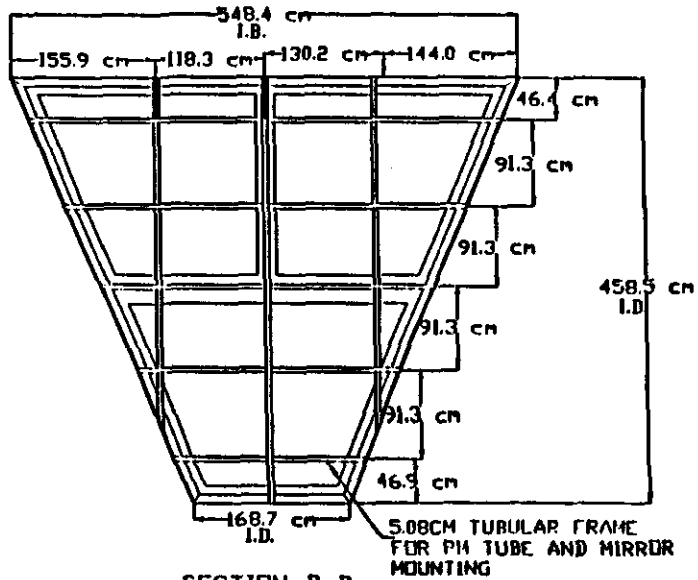

SECTION B-B
(DOWNSTREAM)

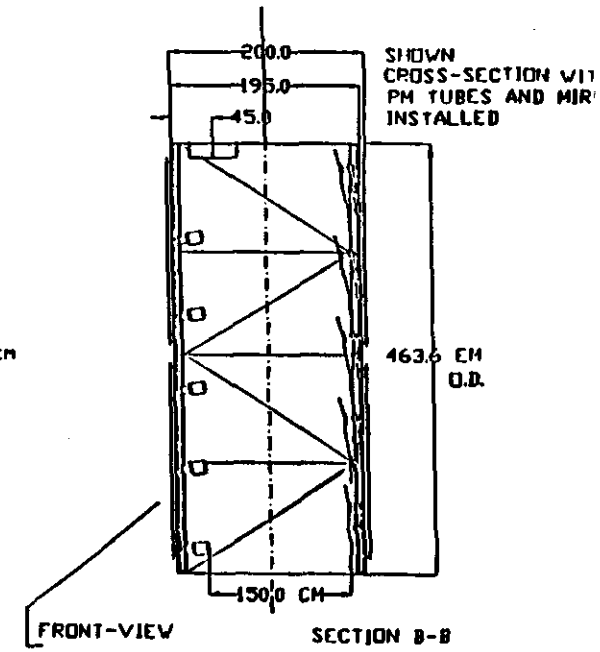

SIDE-VIEW

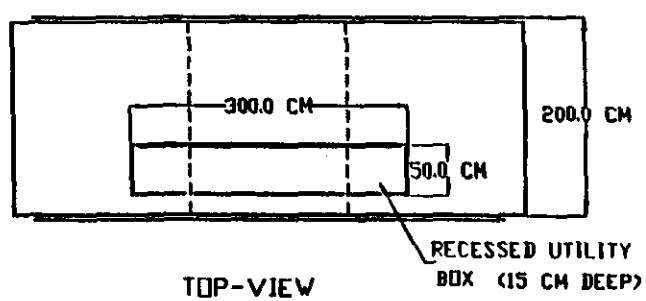

TOP-VIEW

CHERENKOV ENCLOSURE
U. OF COLORADO

NOT TO SCALE

FIG.10

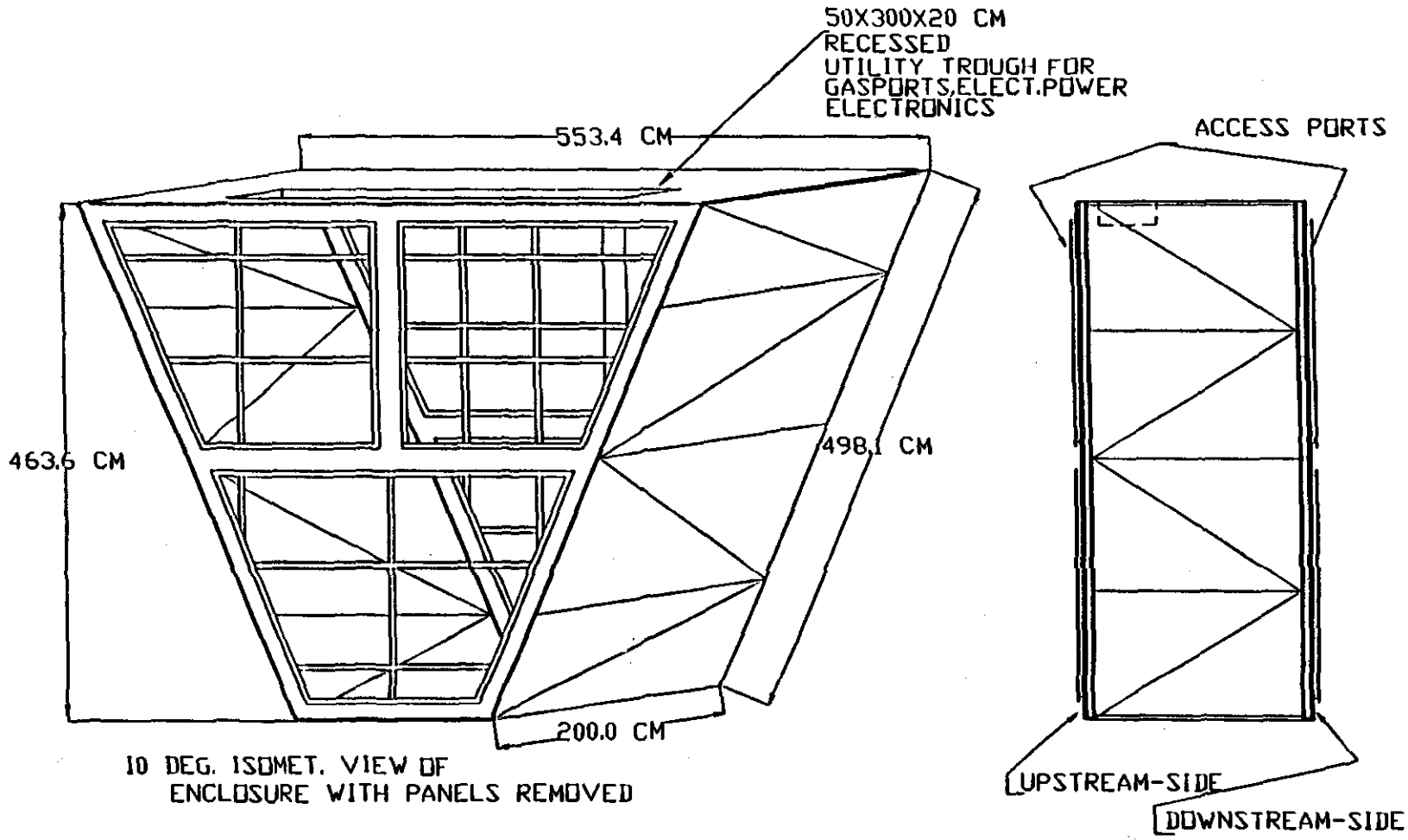

CHERENKOV-MODULE(TYP.)
U. OF COLORADO

NOT TO SCALE

FIG.11

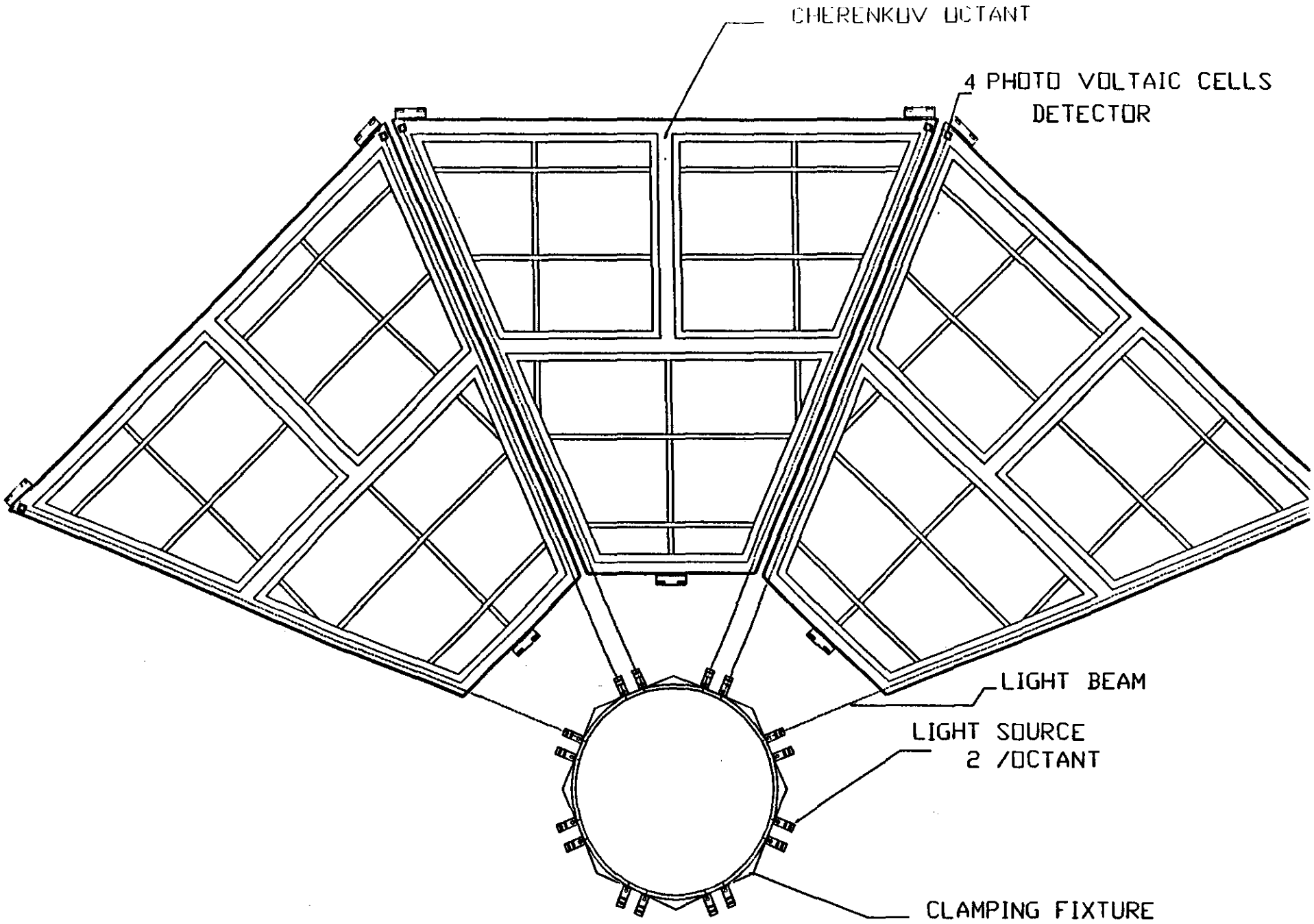

OPTICAL ALIGNMENT SET-UP FIG

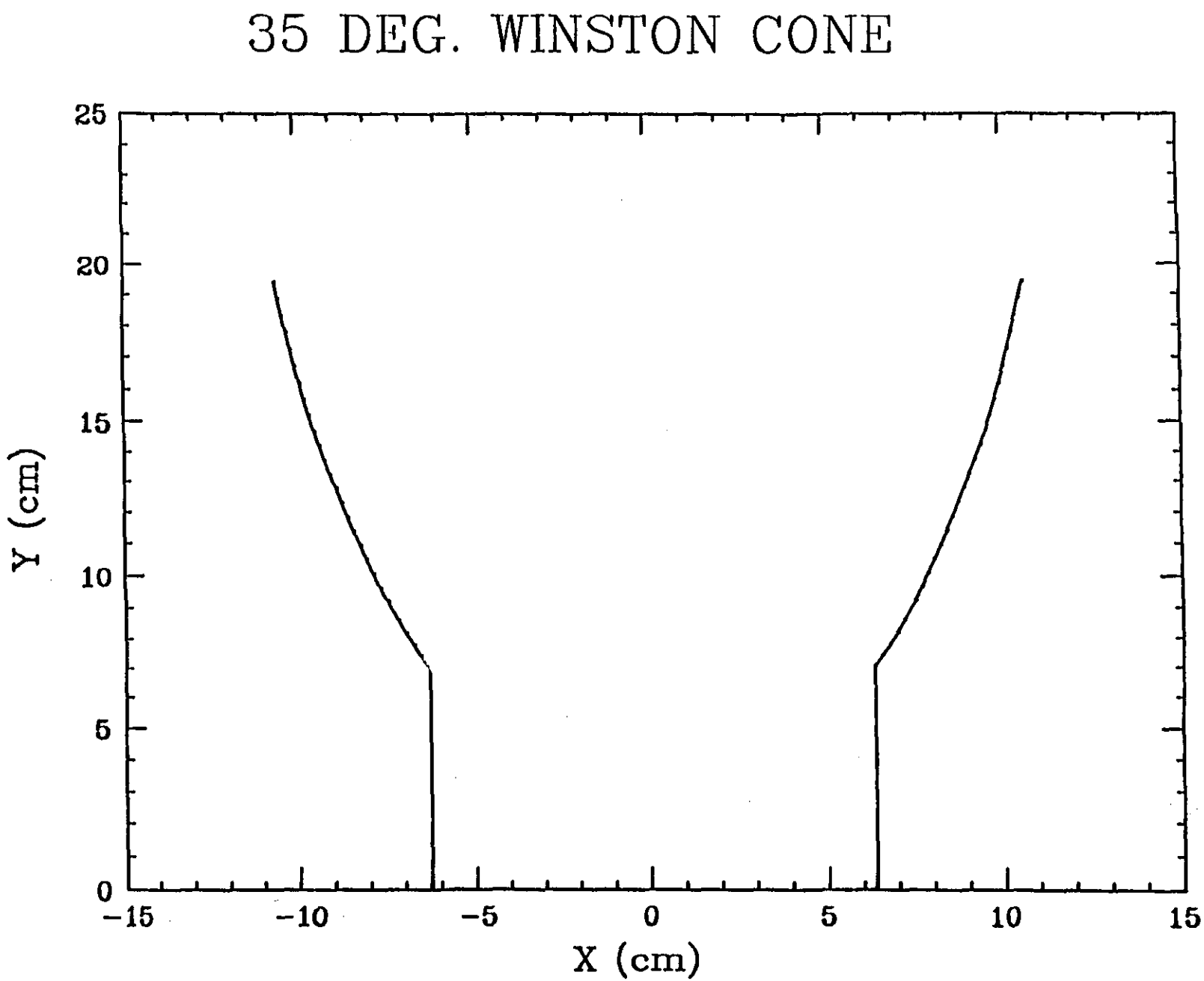

FIG. 13

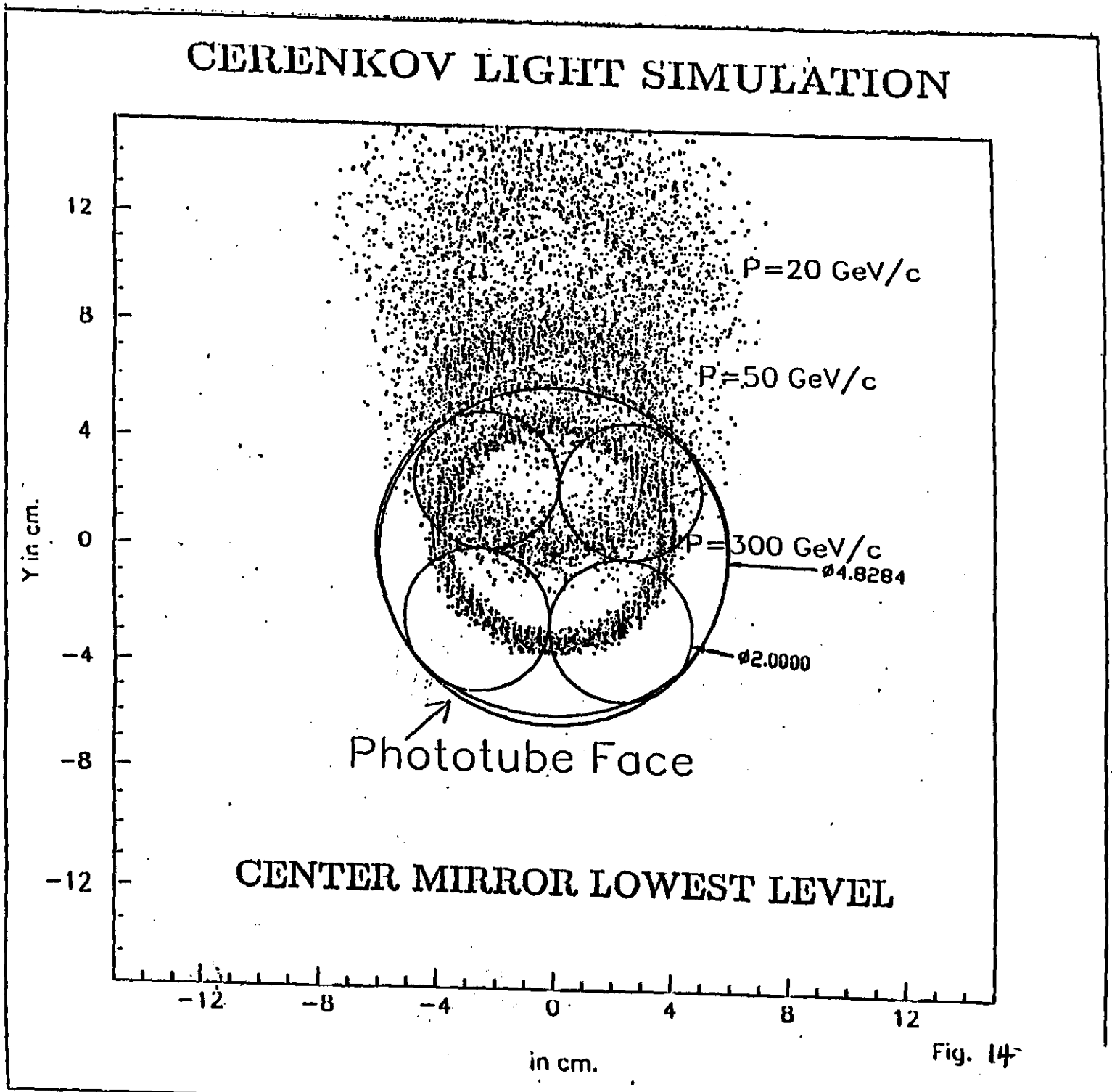
CERENKOV LIGHT SIMULATION
P=20 GeV/c
P=50 GeV/c
P=300 GeV/c
ø4.8284
ø2.0000
Phototube Face
CENTER MIRROR LOWEST LEVEL
Y in cm.
in cm.
12
8
4
0
-4
-8
-12

Fig. 14